



# Microstructure characterization and mechanical properties of (TiC–TiB<sub>2</sub>)–Ni/TiAl/Ti functionally gradient materials prepared by FAPAS



Lifang Hu<sup>a,b,\*</sup>, Daming Chen<sup>a</sup>, Qingsen Meng<sup>a</sup>, Hua Zhang<sup>a</sup>

<sup>a</sup> Department of Materials Science and Engineering, Taiyuan University of Technology, Taiyuan Shanxi 030024, China

<sup>b</sup> Key Laboratory of Interface Science and Engineering in Advanced Materials, Ministry of Education, Taiyuan University of Technology, Taiyuan 030024, China

## ARTICLE INFO

### Article history:

Received 18 November 2014

Received in revised form 27 January 2015

Accepted 29 January 2015

Available online 3 March 2015

### Keywords:

TiC–TiB<sub>2</sub>

TiAl

Combustion synthesis

Shear strength

Wear

## ABSTRACT

The composite ceramics TiC–TiB<sub>2</sub> with Ni as the binder were successfully fabricated and bonded with Ti using TiAl as the transitional layer. (TiC–TiB<sub>2</sub>)–Ni composite ceramics were prepared in-situ through the combustion synthesis process using titanium, nickel and B<sub>4</sub>C powders as raw materials. Interfacial investigations of (TiC–TiB<sub>2</sub>)–Ni/TiAl and TiAl/Ti showed that the three layers were bonded together very well. The TiC and TiB<sub>2</sub> particles of the synthesized composite ceramics were fine and homogeneously dispersed in the matrix. The shear strength increased as the applied current and pressure increased, with the maximum shear strength of the joint reaching 85.78 MPa. The fracture morphology investigated by SEM indicated that the fracture occurred in the (TiC–TiB<sub>2</sub>)–Ni/TiAl interface. The friction coefficient and the loss rate of the ceramic (TiC–TiB<sub>2</sub>)–Ni decreased as the testing temperature increased. The lubrication films of Fe<sub>2</sub>O<sub>3</sub>, TiO<sub>2</sub>, and B<sub>2</sub>O<sub>3</sub> formed at an elevated temperature resulted in a smaller mass loss and friction coefficient.

© 2015 Elsevier B.V. All rights reserved.

## 1. Introduction

TiC and TiB<sub>2</sub> ceramics exhibit a combination of excellent physical and chemical properties, such as high hardness, high melting point, low density, and high corrosion resistance. Due to these excellent properties, in situ synthesized TiC and TiB<sub>2</sub> reinforced metal matrix composites (MMCs) exhibit much better mechanical properties, and have attracted much attention [1–3]. Besides the surface modifications, the synthesized TiC–TiB<sub>2</sub> bulk composite ceramics are very useful, and can be applied in extreme conditions such as high temperature and corrosive environments [4,5]. The composite ceramic TiC–TiB<sub>2</sub> has superior properties including good wear resistance, good wettability, low density and high fracture toughness in comparison with the single phase ceramic [6,7]. Meanwhile, the mechanical properties of the ceramic can be enhanced significantly by adding a certain amount of metals to form the ceramic–metal composites, and it has been reported that Ni, Cr, Fe, Mo, Co and Cu had important role in the sintering process

[8–10]. But in this work, nickel was chosen as the candidate to form the ceramic–metal composite because its melting point is comparable with the TiC–TiB<sub>2</sub> synthesized temperature, and its oxidation resistance is good. Also compare with other metals, nickel can promote the densification of the composite dramatically [11]. (TiC–TiB<sub>2</sub>)–Ni had been produced by various techniques such as powder metallurgy, reaction sintering, hot pressing, high-energy ball milling [12], self propagation high temperature synthesis (SHS) [13] and pressure-assisted thermal explosion reaction [14,15]. Besides the bulk materials, TiC–TiB<sub>2</sub> composite coating can also be prepared by reactive plasma spraying (RPS) [16].

However, like other traditional ceramics, TiC–TiB<sub>2</sub> composites also possess some undesirable properties, such as low toughness and hard to manufacture complicate components. Therefore, it is necessary to bond the ceramics and metals together to meet the engineering requirements. However, the main problem for the bonding process is the residual stress due to the different thermal expansion coefficients of the ceramics and metals in the cooling process, which may result in bonding failure. So the functionally gradient joints between ceramics and metals were put forwards to solve this problem [17].

Field-activated pressure-assisted synthesis (FAPAS) had been successfully employed to fabricate the composite ceramics of

\* Corresponding author at: Department of Materials Science and Engineering, Taiyuan University of Technology, Taiyuan Shanxi 030024, China. Tel.: +86 351 6010520.

E-mail address: [hulifang@tyut.edu.cn](mailto:hulifang@tyut.edu.cn) (L. Hu).

nearly full density. In our previous work, some gradient materials had been prepared successfully by the FAPAS process [18,19]. In this work, the (TiC–TiB<sub>2</sub>)–Ni/TiAl/Ti functionally gradient materials were prepared by this technology. The microstructure of the (TiC–TiB<sub>2</sub>)–Ni composite ceramics were analyzed in detail. The mechanical properties, in particular the shear strength properties of the in-situ combustion synthesized (TiC–TiB<sub>2</sub>)–Ni/TiAl/Ti functionally gradient materials were evaluated, and the wear mechanism of the (TiC–TiB<sub>2</sub>)–Ni was investigated.

## 2. Experimental

The raw materials used in this work included powders of nickel, aluminum, titanium, boron carbide and Ti wafers. All the powders of Ti, Ni, and Al were 99.9% pure and had a particle size of 30–45 μm. The B<sub>4</sub>C powders used in this study had a sieve classification of –325 mesh. The titanium substrates were in the form of disks, 20 mm in diameter and 3 mm thick. All the starting materials were obtained from Alfa Aesar.

Fig. 1 showed the schematic diagram of the green samples. It can be divided into three layers, layer A was the Ti wafer, layer B was a powder mixture of Ti and Al with a molar ratio of 1:1, layer C consisted of Ni, Ti and B<sub>4</sub>C powders, the molar ratio of Ti to B<sub>4</sub>C was 3:1. Layer C was further divided into four parts according to the weight ratio of the Ni. Each mixture with different compositions was first put into an agate bottle to undergo mechanical alloy process for at least 10 h in a planetary mill machine (DQM-0.4L) to ensure homogeneous mixing. Ethanol was used as the grinding medium. Then, the dried powder mixtures were uniaxially cold-pressed, layer by layer, in a graphite mold with 20 mm in inner diameter. During the experiments, TiC and TiB<sub>2</sub> would form by the reaction of Ti and B<sub>4</sub>C, Ni as a binder to make the composites to be dense and compact, and TiAl would form by the reaction of Ti and Al.

The experimental flow chart was described as follows. First, preheated the furnace to 500 °C when the vacuum was below 10.0 Pa, then a current of 1200–1500 A was supplied on the set including the graphite die and the green sample for nearly 30 min until the temperature reaches 1400 °C. The temperature was tested by the thermal couple inserted into the hole of the graphite die. Actually, the internal temperature of the sample was higher than 1400 °C. In the last 5 min, a pressure of 30–60 MPa was imposed on the samples. Then turned off the power, removed the pressure and let the samples cool to room temperature.

The products obtained were characterized in terms of chemical composition and microstructure by a Scanning Electron Microscopy (JEOL JSM-6390) equipped with energy-dispersive spectrometry (EDS). Interfacial microstructure was also analyzed by an optical microscope (OM, ZEISS, Imager. A1). The density of the synthesized samples was measured by Archimedes method.

The shear strength of the synthesized composite ceramics was evaluated in an electronic material testing system (SUSN) with a rate of head movement of 1 mm/min. The samples tested in this work was 7 mm × 7 mm × 9 mm, as shown in Fig. 2. The surface topography of the fractured samples was characterized by SEM.

The wear and friction tests were conducted on a high-velocity wear system (MMS-1G) with a pin-on-disk configuration. The pin was made of (TiC–TiB<sub>2</sub>)–Ni samples with a size of Φ14 mm × 9 mm and the disk was made of GCr15 alloys with a diameter of 16 cm. The hardness of the disk and pin were 760 HV1.0 and 2400 HV1.0 respectively. The wear performance rate was determined by the mass loss per meter. The test temperature ranged from 25 to 400 °C, and the applied load and sliding speed were set as 150 N and 20 m/s respectively. The friction coefficient was determined by the following equation:

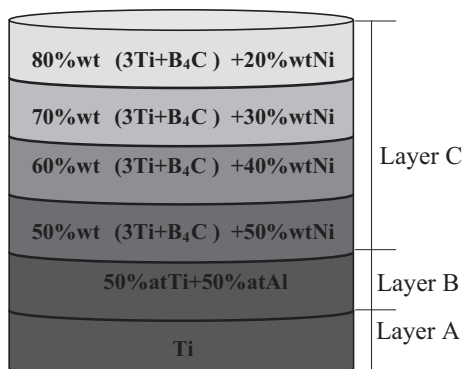


Fig. 1. Schematic diagram of the green sample.

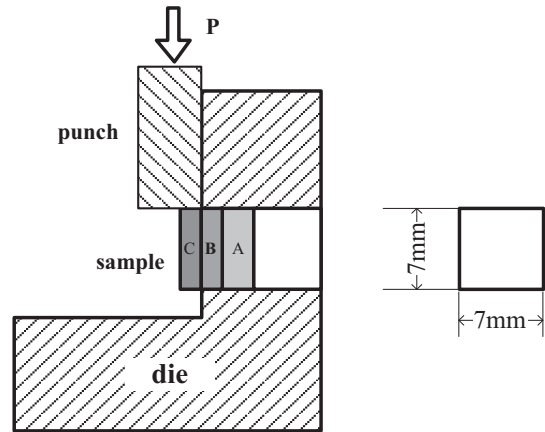


Fig. 2. Schematic diagram of shear strength experiments.

$$\mu = \frac{M}{PR} \quad (1)$$

where  $\mu$  is the friction coefficient,  $M$  the friction torque recorded by a torque recorder,  $P$  is the radial load applied to the sample, and  $R$  is the radius of the friction disk.

## 3. Results and discussions

### 3.1. Microstructure investigations

Fig. 3 showed the cross-sectional SEM images of the samples obtained by the FAPAS process. It can be seen that different layers were bonded together very well, no cracks or defects were found in the interface. A diffusion zone about 500 and 200 μm in width formed between the interface of (TiC–TiB<sub>2</sub>)–Ni/TiAl and TiAl/Ti respectively. The diffusion zone of TiAl/Ti can be divided into two parts, as indicated by the dotted line in Fig. 3 a, part A was characterized by the fine columnar grains, and the columnar grains extended into the TiAl matrix. It can be explained as follows, during the synthesis process, the formation of TiAl from Ti and Al produce a large amount of heat which may promote the melt of the Ti matrix, then the inter diffusion process was accelerated. It can be inferred that the diffusion zone consisted of Ti<sub>3</sub>Al and TiAl. The dramatically inter diffusion was good for improving the bonding strength. The representative microstructure of the (TiC–TiB<sub>2</sub>)–Ni layer (the top layer of the gradient materials) was presented in Fig. 4. Fine grained particles were distributed homogeneously in the matrix, with grain size ranging from 1 to 4 μm, which indicated that a full reaction had been completed during the combustion synthesis process. The gray irregular particles were TiC, and the dark rectangular particles were TiB<sub>2</sub> according to the atomic ratio testing results, as showed in Table 1, nickel enriched along the grain boundaries in white color, the founding was in good agreement with Ni's report [20]. The composites produced by other methods may contain additional compounds, such as TiB, Ni<sub>3</sub>Ti or Ni<sub>3</sub>B. However, in the experiments with the FAPAS technology, composites that only contained TiB<sub>2</sub>, TiC and Ni phases were produced successfully.

Usually, the reaction of Ti with B<sub>4</sub>C was prone to yielding highly porous composites [16]. However, in this study, the synthesized composite ceramics were dense and compact which may be caused by the applied pressure. The microstructure difference was evident for the samples prepared under different applied pressures. Finer specimens characterized by a smaller grain size were observed at samples of 60 MPa, whereas a coarser microstructure was observed in the samples of 30 MPa, as shown in Fig. 4. The pressure clearly had an important effect on the microstructures of the samples. Actually, the density of the synthesized samples prepared

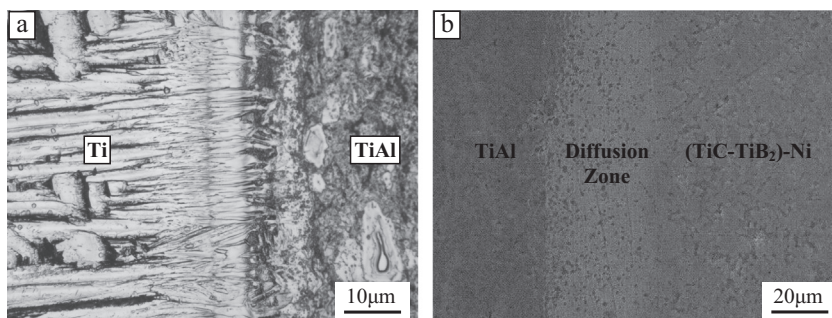


Fig. 3. Cross-sectional SEM images of the interface: (a) Ti and TiAl, (b) TiAl and (TiC-TiB<sub>2</sub>)-Ni.

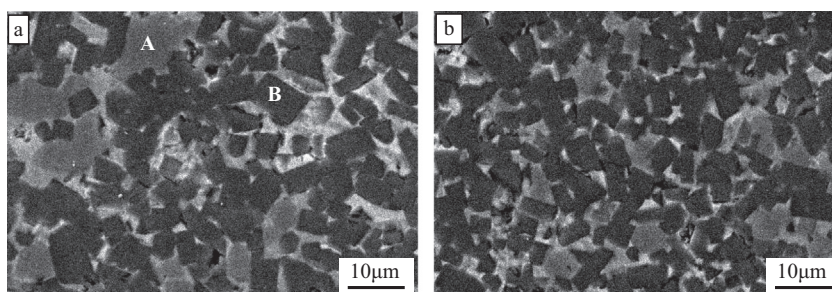


Fig. 4. SEM micrograph of composite ceramics prepared under the current of 1400 A and different pressure of (a) 30 MPa and (b) 60 MPa.

**Table 1**  
EDS results (wt.%) of marked positions in Fig. 4.

Spectrum	B	C	Ti	Ni	Total
A	65.81	0.00	33.98	0.21	100.00
B	0.00	47.57	51.61	0.81	100.00

under 30 and 60 MPa was 4.522 and 5.031 g/cm<sup>3</sup> respectively, which was in good agreement with the microstructure investigations.

The densification process was supposed to be caused by particle rearrangement. It can be explained as follows: actually, the stress imposed on the samples was very uneven, being very high in the regions where the grains were in contact with the punch directly, and very low in the non-contact regions. The pressure at the point of contacts was much larger than the average stress (30–60 MPa) over the whole sample. The stresses at the contact points exceed the fracture stress of the brittle particles of TiC and TiB<sub>2</sub>. Therefore, the TiC and TiB<sub>2</sub> particles continued to be broken up and rearranged. The particles rearrangement led to further densification. In addition, the deformation of the particles at elevated temperatures becomes operational which would promote the densification process.

By examining the SEM morphology closely, it can be seen that the Ni content (in white color) appeared to be lower in the samples prepared with 60 MPa. This phenomenon can be attributed to the loss of the Ni binder, higher applied pressure squeezed Ni out of the samples.

### 3.2. Mechanical properties

The relationship of current intensity and applied pressure on the shear strength was showed in Fig. 5, it indicated that the shear strength increased as the current intensity increased. With the same current intensity, the samples prepared under 60 MPa exhibited higher shear strength. The maximum value reached 85.78 MPa

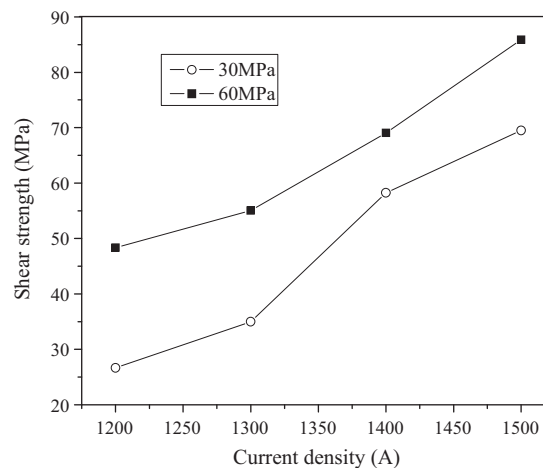
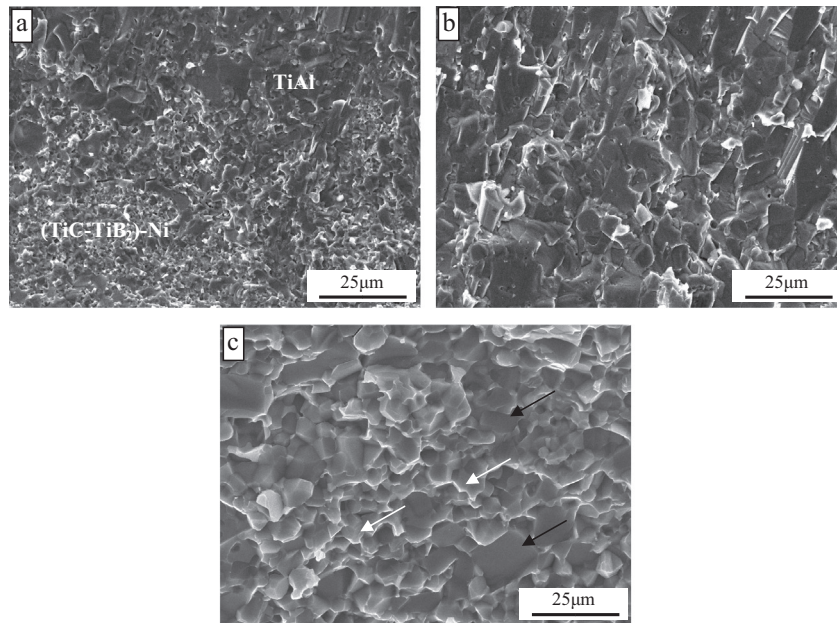


Fig. 5. Effect of current and pressure on shear strength of the samples.

under 1500 A and 60 MPa. It can be indicated that the current intensity and applied pressure directly affected the shear strength. It has been proven by Huang et al. [21,22] that the refined microstructure and improved homogeneity resulted in remarkable improvement of shear strength, due to the fracture mechanism changing from crack bridging to subsequent pullout. Since the applied pressure had reached 60 MPa, the size and distribution of TiC and TiB<sub>2</sub> particles became much smaller and uniform in the synthesized ceramics. Fine grains lead to much more grain boundaries, which can impede the propagation of cracks by the mechanism of crack deflection, thus absorbing much energy of the microcrack propagation. Larger grain size was detrimental to the fracture toughness of the composite ceramics [17]. Moreover, it is assumed that the diffusion zone increased as the current intensity increased which can also improve the mechanical properties. It can be inferred that both of the current density and the pressure determined the shear strength of the samples.



**Fig. 6.** SEM images of the fractured sample prepared under 60 MPa: (a) (TiC–TiB<sub>2</sub>)–Ni/TiAl interface, (b) TiAl, and (c) (TiC–TiB<sub>2</sub>)–Ni.

The fracture morphology of the samples prepared under different pressures was compared. Both samples prepared under the pressure of 30 MPa and 60 MPa fractured at the (TiC–TiB<sub>2</sub>)–Ni/TiAl interface, as seen in Fig. 6. It can be inferred that the weakness of the gradient materials occurred at the bonding interface of (TiC–TiB<sub>2</sub>)–Ni/TiAl.

Fracture morphology showed that a mixed fracture mode of intergranular fracture and transgranular fracture was present. For TiB<sub>2</sub> particles, their fracture modes were related to their crystal orientation. If the TiB<sub>2</sub> particles grew parallel to the shear direction, intergranular fracture tended to occur, as shown by the black arrow in Fig. 6c, while transgranular fracture would occur when the crystal orientation was vertical to the shear direction, as shown by the white arrow in Fig. 6c.

### 3.3. Wear behavior at elevated temperature

The synthesized composites was aim to be used at high temperature environments. So the wear rate and average friction

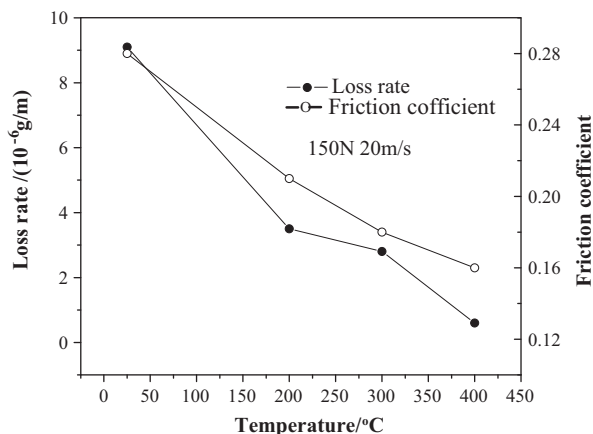


**Fig. 7.** Temperature effects on the wear rate and friction coefficient of the synthesized ceramics.

coefficient of the synthesized composite ceramics at elevated temperatures were investigated. Both the wear rate and the average friction coefficients decreased as the temperature increased, as showed in Fig. 7. In order to investigate the wear mechanisms of the synthesized composite ceramics in sliding against GCr15, the morphologies and the elemental composition of the sliding surfaces after wear tests at different temperatures were analyzed.

It can be seen from Fig. 8a that a film was formed on the sliding surface with some microploughing scratches on it, moreover, the worn surface was characterized by some cracks and craters. However, at higher temperature, the sliding surface was characterized by a compact film with some craters, as showed in Fig. 8b. Compare the two pictures, it can be seen that the film formed on the surface was much smoother at higher temperature.

The differences of the two pictures and the wear mechanism can be explained as follows: due to the applied load, the GCr15 disk surfaces and contact asperities of the samples undergo deformation, the asperities of the GCr15 disk as well as TiC and TiB<sub>2</sub> particles detached from the substrate which led to adhesion. Also some Fe would be transferred from the GCr15 disk to the ceramics. At room temperature, these asperities and detached ceramic particles would be smashed into powders. Some powders left the sliding surface which lead to mass loss and some powders adhered to the sliding surface and acted as grinding medium which may promote the wear process, as showed in Fig. 8a.

Compared the EDS test results, it can be known that both the worn surfaces contain much O which indicated oxides formed due to the friction heat during the wear process. However, at elevated temperatures, these powders were oxidized and melted quickly to form smooth and compact lubricant film, as showed in Fig. 8b, which can decrease the friction coefficients and mass loss dramatically. The particle TiB<sub>2</sub> was oxidized to TiO<sub>2</sub> and B<sub>2</sub>O<sub>3</sub>, and Fe was oxidized to Fe<sub>2</sub>O<sub>3</sub>, as showed in Fig. 9. The melting point of B<sub>2</sub>O<sub>3</sub> is very low, only 445 °C, its easily to be molten. So B<sub>2</sub>O<sub>3</sub> facilitated the formation of the molten film, and the molten film wrapped on the worn surface can protect the substrate from further oxidation. According to Table 2, the molten film contained more B, so the lubricant film formed at elevated temperatures contain more B<sub>2</sub>O<sub>3</sub>. Formation of B<sub>2</sub>O<sub>3</sub> can decrease the friction

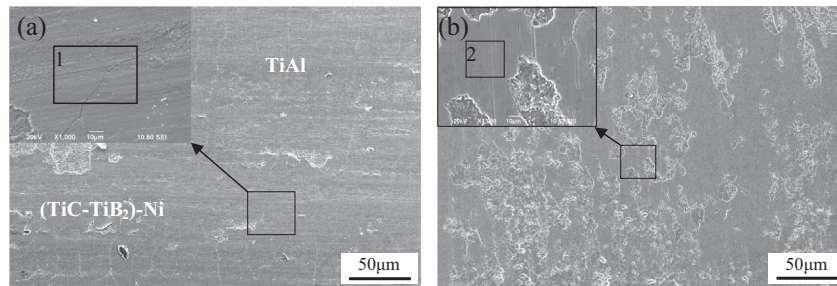


Fig. 8. SEM images of the worn surface at 400 °C, 150 N, and 20 m/s with positions for collection of the EDS in Table 2: (a) 25 °C and (b) 400 °C.

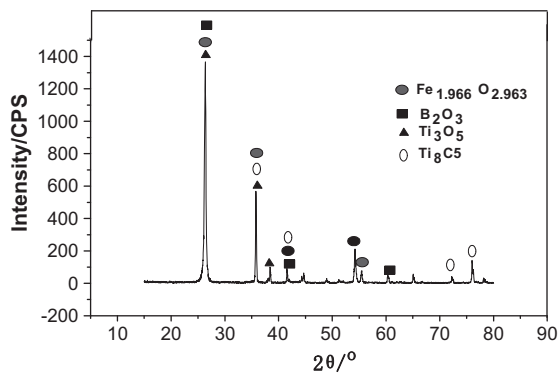


Fig. 9. XRD pattern of the worn surface tested at 400 °C.

Table 2  
EDS results (wt.%) of marked positions on the worn surface (Fig. 8).

Spectrum	B	C	O	Ti	Cr	Fe	Ni	Total
1	4.81	4.04	34.62	23.60	0.59	31.60	0.75	100.00
2	13.28	7.41	22.14	19.53	0.61	31.45	5.57	100.00

coefficient and mass loss. Because of the small shear strength, some molten films would be peeled off easily and craters would be formed. It can be concluded that the synthesized ceramics had excellent wear-resistance at elevated temperatures due to the formation of the molten lubricant film. The cracks appeared at room temperature may be led by the different thermal expansion properties of TiC and TiB<sub>2</sub> particles, however, at higher temperature, the cracks were covered by the molten film and cannot be detected.

#### 4. Conclusions

- (1) The composite ceramics TiC–TiB<sub>2</sub> with Ni as the binder were successfully fabricated and bonded with Ti using TiAl as the transitional layer. In this work, a significant refinement of the grain size of the ceramic phases was observed at the samples under a higher pressure.
- (2) Shear experiments showed that fractures occurred at the (TiC–TiB<sub>2</sub>)–Ni/TiAl interface. Higher pressure and current density led to a remarkable increase of the shear strength. Meanwhile, due to higher applied pressure, the refined microstructure and improved homogeneity of the composites were achieved in this work.
- (3) Friction testing results showed that the composite ceramics had a better wear-resistance at elevated temperatures due to the formation of the molten lubricant film consisting of TiO<sub>2</sub>, B<sub>2</sub>O<sub>3</sub> and Fe<sub>2</sub>O<sub>3</sub>.

#### Acknowledgements

This project was supported by the National Natural Science Foundation of China (51405328). We would like to thank T.C. Scott in helping prepare this paper. T.C. Scott is supported in China by the project GDW201400042 for the “high end foreign experts project”.

#### References

- [1] J. Xu, B. Zou, X. Fan, S. Zhao, Y. Hui, Y. Wang, X. Zhou, X. Cai, S. Tao, H. Ma, X. Cao, Reactive plasma spraying synthesis and characterization of TiB<sub>2</sub>–TiC–Al<sub>2</sub>O<sub>3</sub>/Al composite coatings on a magnesium alloy, *J. Alloys Comp.* 596 (2014) 10–18.
- [2] Ö. Balci, D. Ağaoğulları, H. Gökçe, İ. Duman, M.L. Öveçoğlu, Influence of TiB<sub>2</sub> particle size on the microstructure and properties of Al matrix composites prepared via mechanical alloying and pressureless sintering, *J. Alloys Comp.* 586 (2014) S78–S84.
- [3] B. Du, S.R. Paital, N.B. Dahotre, Synthesis of TiB<sub>2</sub>–TiC/Fe nano-composite coating by laser surface engineering, *Opt. Laser Technol.* 45 (2013) 647–653.
- [4] Binglin Zou, Ping Shen, Zhongming Gao, Qichuan Jiang, Combustion synthesis of TiC<sub>x</sub>–TiB<sub>2</sub> composites with hypoeutectic, eutectic and hypereutectic microstructures, *J. Eur. Ceram. Soc.* 28 (2008) 2275–2279.
- [5] H. Zhao, Y.B. Cheng, Formation of TiB<sub>2</sub>–TiC composites by reactive sintering, *Ceram. Int.* 25 (1999) 353–358.
- [6] D. Vallauri, I.C. Atías Adrián, A. Chrysanthou, TiC–TiB<sub>2</sub> composites: a review of phase relationships, processing and properties, *J. Eur. Ceram. Soc.* 28 (2008) 1697–1713.
- [7] A. Farid, S. Guo, F.-E. Cui, P. Feng, T. Lin, TiB<sub>2</sub> and TiC stainless steel matrix composites, *Mater. Lett.* 61 (2007) 189–191.
- [8] X. Zhang, C. Hong, J. Han, H. Zhang, Microstructure and mechanical properties of TiB<sub>2</sub>/(Cu, Ni) interpenetrating phase composites, *Scr. Mater.* 55 (2006) 565–568.
- [9] D. Ağaoğulları, H. Gökçe, İ. Duman, M.L. Öveçoğlu, Influences of metallic Co and mechanical alloying on the microstructural and mechanical properties of TiB<sub>2</sub> ceramics prepared via pressureless sintering, *J. Eur. Ceram. Soc.* 32 (2012) 1949–1956.
- [10] Meilin Gu, Chuanzhen Huang, Bin Zou, Binqiang Liu, Effect of (Ni, Mo) and TiN on the microstructure and mechanical properties of TiB<sub>2</sub> ceramic tool materials, *Mater. Sci. Eng., A* 433 (2006) 39–44.
- [11] J. Jaroszewicz, A. Michalski, Preparation of a TiB<sub>2</sub> composite with a nickel matrix by pulse plasma sintering with combustion synthesis, *J. Eur. Ceram. Soc.* 26 (2006) 2427–2430.
- [12] B. Zou, C. Huang, J. Song, Z. Liu, L. Liu, Y. Zhao, Effects of sintering processes on mechanical properties and microstructure of TiB<sub>2</sub>–TiC+8 wt% nano-Ni composite ceramic cutting tool material, *Mater. Sci. Eng., A* 540 (2012) 235–244.
- [13] Y.F. Yang, Q.C. Jiang, Reaction behaviour, microstructure and mechanical properties of TiC–TiB<sub>2</sub>/Ni composite fabricated by pressure assisted self-propagating high-temperature synthesis in air and vacuum, *Mater. Des.* 49 (2013) 123–129.
- [14] D. Vallauri, F.A. Deorsola, Synthesis of TiC–TiB<sub>2</sub>–Ni cermets by thermal explosion under pressure, *Mater. Res. Bull.* 44 (2009) 1528–1533.
- [15] Y.F. Yang, D.K. Mu, Q.C. Jiang, A simple route to fabricate Ti–TiB<sub>2</sub>/Ni composite via thermal explosion reaction assisted with external pressure in air, *Mater. Chem. Phys.* 143 (2014) 480–485.
- [16] B. Zou, S. Tao, W. Huang, Z.S. Khan, X. Fan, L. Gu, Y. Wang, J. Xu, X. Cai, H. Ma, X. Cao, Synthesis and characterization of in situ TiC–TiB<sub>2</sub> composite coatings by reactive plasma spraying on a magnesium alloy, *Appl. Surf. Sci.* 264 (2013) 879–885.
- [17] X. Huang, Z. Zhao, L. Zhang, Fusion bonding of solidified TiC–TiB<sub>2</sub> ceramic to Ti–6Al–4V alloy achieved by combustion synthesis in high-gravity field, *Mater. Sci. Eng., A* 564 (2013) 400–407.

- [18] S.P. Chen, Q.S. Meng, J.F. Zhao, Z.A. Munir, Synthesis and characterization of TiB<sub>2</sub>-Ni-Ni<sub>3</sub>Al-CrNi alloy graded material by field-activated combustion, *J. Alloys Comp.* 476 (2009) 889–893.
- [19] Shaoping Chen, Qingsen Meng, Nan Zhang, Pengfei Xue, Zuhair A. Munir, In situ synthesis and bonding of Ti-TiAl-TiC/Ni functionally graded materials by field-activated pressure-assisted synthesis process, *Mater. Sci. Eng., A* 538 (2012) 103–109.
- [20] D.R. Ni, L. Geng, J. Zhang, Z.Z. Zheng, TEM characterization of symbiosis structure of in situ TiC and TiB prepared by reactive processing of Ti-B<sub>4</sub>C, *Mater. Lett.* 62 (2008) 686–688.
- [21] X. Huang, L. Zhang, Z. Zhao, C. Yin, Microstructure transformation and mechanical properties of TiC-TiB<sub>2</sub> ceramics prepared by combustion synthesis in high gravity field, *Mater. Sci. Eng., A* 553 (2012) 105–111.
- [22] X. Huang, Z. Zhao, L. Zhang, C. Yin, J. Wu, Microstructure modification and fracture behavior of solidified TiC-TiB<sub>2</sub> ceramic prepared by combustion synthesis in ultra-high gravity field, *J. Asian Ceram. Soc.* 2 (2014) 144–149.